research articles Journal of proteome research

Comparative Proteomic Expression Profile in All-*trans* Retinoic Acid Differentiated Neuroblastoma Cell Line

Flora Cimmino, Daniela Spano, Mario Capasso, Nicola Zambrano, Roberta Russo, Massimo Zollo, and Achille Iolascon*

Dipartimento di Biochimica e Biotecnologie Avanzate, Universita'di Napoli Federico II, Centro di Ingegneria Genetica CEINGE- Biotecnologie Avanzate, Napoli, Italy

Received December 29, 2006

Neuroblastoma (NB) is an infant tumor which frequently differentiates into neurons. We used two-dimensional differential in-gel electrophoresis (2D-DIGE) to analyze the cytosolic and nuclear protein expression patterns of LAN-5 cells following neuronal differentiating agent all-*trans*-retinoic acid treatment. We identified several candidate proteins, from which Gβ2 and Prefoldin 3 may have a role on NB development. These results strength the use of proteomics to discover new putative protein targets in cancer.

Keywords: neuroblastoma • all-*trans*-retinoic acid • 2D-DIGE • LAN-5 human neuroblastoma cell line

Introduction

Neuroblastoma (NB) is manifested in childhood as an extracranial solid tumor of the sympathetic nervous system that can show extraordinary clinical and biological heterogeneity.[1] The majority of NBs are aggressive metastatic tumors with poor clinical outcome, despite intensive multimodal therapy. The most favorable subset of this embryonic tumor (stage 4S) can spontaneously differentiate or regress to a benign tumor phenotype, even after no, or minimal, therapy.[2−4] This has generated considerable interest in agents that are able to regulate these important biological processes.

Vitamin A and its analogues (the retinoids) have roles in cell proliferation, differentiation, and apoptosis in normal tissues during embryonic development.[4] It has also been shown that retinoic acid can restore "normal" functions (differentiation) in certain tumors, such as NB,[5] melanoma,[6] and acute promyelocytic leukemia (PML).[7] In clinical practice, all-*trans* retinoic acid (ATRA) is mainly used for patients with acute PML.[8] In the treatment of NB patients, ATRA has been used as a chemotherapeutic agent with some success,[9] but 13*cis*-RA is preferred due to its more favorable pharmacokinetics.[10−12] Furthermore, studies comparing the activities of 13*cis*-RA and ATRA in NB cell lines have demonstrated similar potencies of these retinoids, in terms of cellular differentiation, growth arrest, and regulation of tumor markers such as MYCN.[13]

RA effects appear to be mediated by two families of nuclear retinoic acid receptors (RARs and RXRs) that form a part of the steroid/thyroid/vitamin D superfamily.[14] These receptors function as homo/heterodimers and directly modulate transcriptional activity by binding to the RA response elements (RAREs). RA affects NB differentiation either through the transcriptional regulation of genes directly involved in the differentiation process or that control the differentiation process.[5,15] Over the past two decades, a large number of NB cell lines have been generated, which have diverse biological characteristics. These NB cells provide "good" model systems both for the unraveling of the molecular basis of NB development, and for the development of therapeutic protocols based on NB differentiation.

Recently, there has been significant progress in the development of systematic approaches to study NB development, at both the transcriptional and translational levels. Gene expression profiling on NB specimens have been described as identifying the molecular signatures of high-risk and low-risk tumors[16−18] and novel prognostic markers.[19−21] The search for markers at the transcriptional level is less reliable than at the protein level, as there is a "long" and unpredictable route from RNA to proteins, and very often protein expression does not correlate with mRNA expression. Indeed, several proteins can be encoded by the same gene, through splice variants and post-translational modifications that cannot be directly predicted from gene sequence. The most commonly used comparative proteomic approach is two-dimensional difference gel electrophoresis (2D-DIGE) coupled with mass spectrometry (MS), which provides a good proteomic tool for the investigation of novel proteins that might serve as candidates for tumor markers. Previously, 2D-PAGE analyses of protein changes were performed to study chemoresistance,[22] to search for markers for tumor diagnosis in NB cell lines,[23,24] and to study quantitatively and qualitatively differences in healthy and pathological NB mouse samples.[25,26] Moreover, proteomic characterization of differentiation induced by ATRA has been described in promyelocytic cells[7,27,28] and in mouse embryonic stem cells.[29] However, very little is known about the large-scale protein

* Corresponding author: Achille Iolascon, Full Professor of Medical Genetics. Dipartimento di Biochimica e Biotecnologie Avanzate, Universita'di Napoli Federico II; Centro di Ingegneria Genetica CEINGE-Biotecnologie Avanzate, via Comunale Margherita 482, 80145-Napoli, Tel., +39 081 3737 897; fax, +39 081 3737 804; e-mail, iolascon@ceinge.unina.it.

components of early stage differentiation of NB cell lines into neural cells by ATRA.

Recently, 2D-DIGE has shown advantages over traditional 2D-PAGE for several aspects: (1) multiple pre-labeling of samples; (2) introducing a pooled internal standard; (3) co-detection; and (4) a wider dynamic range. This technology[30] has been successfully applied to identify potential biomarkers of various cancers, such as colon cancer,[31] oesophageal carcinoma,[32] and breast cancer.[33] In spite of this, one of the limitations of DIGE-based proteomics is the low identification rate of low-abundance proteins.[34]

To gain further insight into the molecular mechanisms of NB differentiation induced by ATRA, we have combined the 2D-DIGE proteomic approach and the advantages of subcellular fractionation of the LAN-5 cell line proteome in cytosolic and nuclear fractions, in response to ATRA treatment in a time course analysis. We detected significantly modulated expression of 126 protein spots: 58 in the cytosolic fraction and 68 in the nuclear fraction. We identified 33 differentially expressed proteins from 38 picked spots and have validated some protein expression patterns in biologically different NB cell lines, indicating a common pattern of regulation. Further investigations of these candidate markers using functional assays and careful studies of many patients should lead to the identification of markers that can be used clinically and may provide insights into the mechanisms of NB differentiation.

Materials and Methods

Cell Culture and Neuronal Differentiation. The human LAN-5 NB cell line was grown in RPMI medium supplemented with 10% heat-inactivated fetal bovine serum (FBS), 100 kU/L penicillin, and 100 mg/L streptomycin, at 37 °C, in 5% CO_2 in a humidified atmosphere. The human SK−N-BE and SH-SY5Y NB cell lines were grown in Dulbecco's modified Eagle's medium supplemented with 10% heat-inactivated FBS, 100 kU/L penicillin and 100 mg/L streptomycin, at 37 °C, in 5% CO_2 in a humidified atmosphere. The cells were passaged 1:4 twice weekly and routinely fed 24 h before each experiment.

Neuronal differentiation was induced in cells at 80% confluence by 5 μM ATRA (Sigma) dissolved in dimethyl sulfoxide (DMSO). All experiments were performed under dim light, and the tubes containing retinoids were wrapped in aluminum foil.

The cells were washed three times in 10 mL ice-cold phosphate-buffered saline (PBS) and harvested 0, 8, 24, and 48 h after RA treatment, using a cell scraper. This time course was chosen to reflect primary or early responses of NB cell lines to the RA treatment. Each experiment was performed in triplicate. Three cellular plates for each experimental point (0, 8, 24, and 48 h) were harvested, pooled, and centrifuged for 5 min at 2000*g* at 4 °C. The pellets were frozen at −80 °C until sample preparation.

Sample Preparation. 1. Cytosolic Protein Fraction Preparation. The cell pellets were incubated on ice in ice-cold lysis buffer (250 mM sucrose, 3 mM imidazole, pH 7.4, and 1 mM EDTA) in the presence of a protease inhibitor cocktail (Complete Mini EDTA-free, Roche). The cellular pellets were disrupted by 8−10 passes through a 22-guage needle, and then centrifuged at 16 000*g* for 20 min at 4 °C. The pellets obtained were considered as the nuclear fraction, while the post-nuclear supernatant (PNS) contained the cytosolic fraction and cell membranes. The nuclear pellet was used for preparation of the nuclear extract.

The PNS was ultracentrifuged at 100 000*g* for 45 min at 4 °C. The supernatant obtained here was used as the cytosolic fraction. The cytosolic fraction was solubilized in 7 M urea, 2 M tiourea, 40 mM Tris-HCl, and 4% CHAPS and incubated for 30 min under agitation at room temperature.

2. Nuclear Protein Fraction Preparation. The nuclear pellet obtained above was resuspended in 7 M urea, 2 M tiourea, 40 mM Tris-HCl, pH 8.5, 0.24% Triton X-100, and 4% CHAPS. After 30 min of incubation at room temperature, 10 mM spermine was added, and the solution was incubated for 1 h at room temperature. The precipitated material was removed by ultracentrifugation at 100 000*g* for 45 min at 4 °C.

The solubilized cytosolic and nuclear fractions were reduced by 5 mM tributylphosphine (TBP) for 90 min and were alkylated by 10 mM iodacetamide (IAA) for 90 min, in tubes wrapped in aluminum foil. After, the samples were precipitated for 90 min in a mix of acetone/methanol (8:1) at −20 °C and centrifuged at 13 400*g* for 30 min, at 4 °C. The pellets were air-dried and solubilized in 7 M urea, 2 M tiourea, 3% CHAPS, and 30 mM Tris-HCl.

Protein concentrations were determined using the Bradford method (Bio-Rad).

Cy-Dye Labeling of Cytosolic and Nuclear Fraction Extracts. The pH of the samples was adjusted to pH 8.5 with 0.1 M NaOH or HCl. Typically, 50 μg of extract was labeled with 400 pmol Cy2 (standard mixture of extracts), Cy3, and Cy5 (untreated and RA-treated cells). The labeling reaction was carried out on ice in the dark for 30 min, and was stopped with 1 mM lysine (final concentration). The samples were then mixed, and supplemented with 0.5% carrier ampholytes pH 3−10 (Bio-Rad) and 1% bromophenol blue. The final volume was adjusted to 380 μL with 7 M urea, 2 M tiourea, and 3% CHAPS.

2-D Gel Electrophoresis, Imaging, and DIGE Analysis. The immobilized pH gradient IPG gel strips (length, 17 cm; thickness, 0.5 mm), nonlinear pH gradient range (NL) pH 3−10 (Bio-Rad) were passively rehydrated with 150 μg of tripartite-labeled sample (50 μg for each labeled sample and 50 μg internal standard) in the dark overnight. Isoelectric focusing (IEF) was carried out with a Protean IEF Cell (Bio-Rad), with a low initial linear voltage up to 1000 V in 5 h, and then by applying a voltage gradient up to 10 000 V with a limiting current of 50 μA/strip. The total product time × voltage applied was 76 000 V/h for each strip, and the temperature was set to 20 °C. The strips were equilibrated in 6 M urea, 2% SDS, 20% glycerol, and 0.375 M Tris-HCl (pH 8.8), for 30 min in the dark.

Equilibrated IPG strips were transferred onto 18 × 20-cm 11% polyacrilamide gels, within low-fluorescence glass plates (ETTAN-DALT, GE Healthcare). The second-dimension SDS-PAGE was performed using a Peltier-cooled DALT II electrophoresis unit (GE Healthcare) at 1 W/gel overnight. The gels were scanned with a Typhoon 9400 variable mode imager (GE Healthcare) using mutually exclusive excitation/emission wavelengths for Cy2 (488 nm/520 nm), Cy3 (532 nm/580 nm), and Cy5 (633 nm/670 nm). Images were normalized and analyzed for statistics, and differentially expressed spots were quantified using the DeCyder 5.0 software (GE Healthcare).

A DeCyder differential in-gel-analysis (DIA) module was used for pairwise comparisons of each sample (Cy3 and Cy5) to the Cy2 mixed standard present in each gel. The DeCyder biological variation analysis (BVA) module was then used to simultaneously match all of the protein-spot maps from the gels, and to calculate average abundance ratios across triplicate samples.

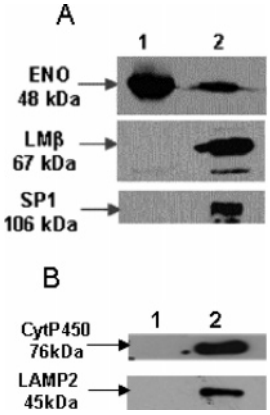

Figure 1. Western blotting was performed to test the cross-contamination of cytosolic (lane 1) and nuclear (lane 2) protein extracts from the LAN-5 NB cell line. (A) The biochemical protein markers used for the nuclei were anti-LMβ and anti-SP1 antibodies, and an anti-ENO antibody was used for the cytosolic fraction. (B) To check organelles enrichment in both fractions, cytochrome P450 and LAMP-2 proteins were used as marker of mitochondria and lysosomes, respectively.

Table 1. Experimental Design of 2D-DIGE[a]

		gel n*o*.	Cy2	Cy3	Cy5
1 Experiment	{	1	pooled standard	0 h	8 h
		2	pooled standard	24 h	48 h
2 Experiment	{	3	pooled standard	0 h	8 h
		4	pooled standard	24 h	48 h
3 Experiment	{	5	pooled standard	8 h	0 h
		6	pooled standard	48 h	24 h

[a] Scheme of labeling used for cytosolic and nuclear extracts.

Proteins with molecular masses from approximately 20−150 kDa were resolved, and approximately 3000 spots/gel were detected using the DeCyder image analysis software. To avoid false positives, only spots with a fold change equal or above 1.3 and a p value $\leq$0.075 (Student's t test) were taken in account. A manual sorting based on the quality of the protein spots was also performed.

Protein Identification by MS. For preparative protein separations, 1 mg of unlabeled sample was used to passively rehydrate the IPG strips. The first and second dimension runs were conducted as described above. After 2-D electrophoresis, the separated proteins were visualized using the universal staining methods of anionic dyes (Coomassie Colloidal Blue; Pierce). The resolved polypeptides were fixed in 10% acetic acid/40% methanol solution for 12−16 h before staining. The staining in Colloidal Coomassie was performed for 3 days, and then the gels were washed three times in deionized H_2O. Selected protein spots were excised from the gels and washed in 50 mM ammonium bicarbonate, pH 8.0, in 50% acetonitrile until completely distained. The gel pieces were re-suspended in 50 mM ammonium bicarbonate, pH 8.0, containing 100 ng of trypsin, and incubated for 2 h at 4 °C and overnight at 37 °C. The supernatants containing the resulting peptide mixtures were removed, and the gel pieces were re-extracted with acetonitrile. The two fractions were then collected and freeze-dried.

1. MALDI MS Analysis. MALDI mass spectra were recorded on an Applied Biosystem Voyager DE-PRO mass spectrometer equipped with a reflectron analyzer and used in delayed extraction mode. One microliter of peptide sample was mixed

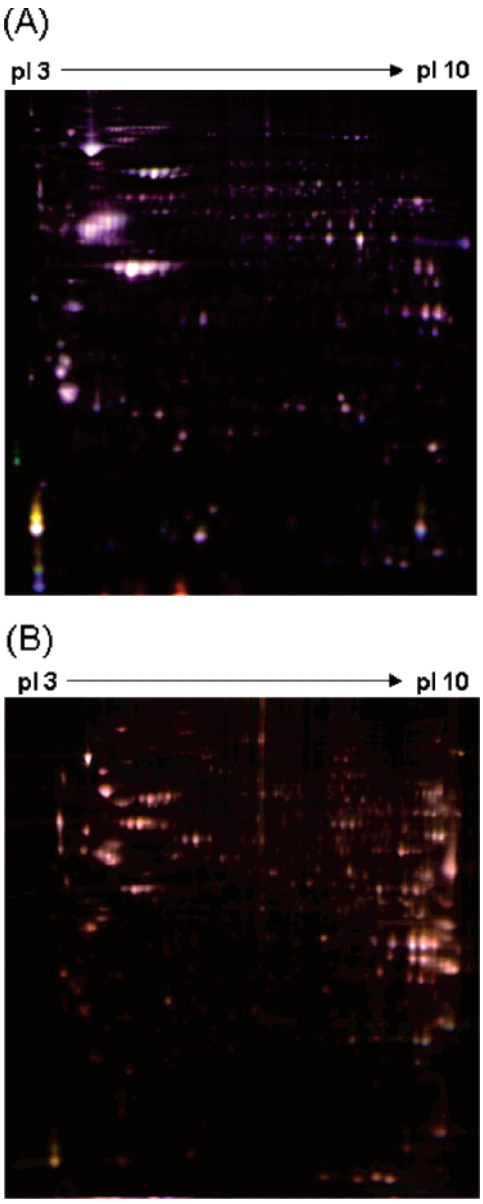

Figure 2. Isoelectric focusing was performed on immobilized pH gradient IPG gel strip, NL pH 3−10, and the proteins were further separated by 11% SDS-PAGE in the second dimension. (A) Overlaid images of Cy3- and Cy5-labeled cytosolic protein extracts; and (B) as for panel A, for a nuclear protein extracts.

with an equal volume of α-cyano-4-hydroxycynnamic acid as matrix (10 mg/mL in 0.2% trifluoroacetic acid (TFA) in 70% acetonitrile), applied to the metallic sample plate, and air-dried. Mass calibration was performed using the standard mixture provided by the manufacturer. Mass signals were then used for database searching using the MASCOT peptide fingerprinting search program (Matrix Science, Boston, MA), available on the Internet.

2. LC−MS/MS Analysis. The unknown protein spots from peptide mass fingerprinting were further analyzed by LC−MS/MS using a Q-TOF Ultima hybrid mass spectrometer (Micromass, Waters) equipped with a Z-spray source and coupled online with a capillary chromatography system (CapLC, Waters). The peptide mixture (10 μL) was first loaded onto a reverse-phase trap-column (Waters) at 10 μL/min using 0.2% formic acid as eluent. The sample was then transferred to a C_{18} reverse-

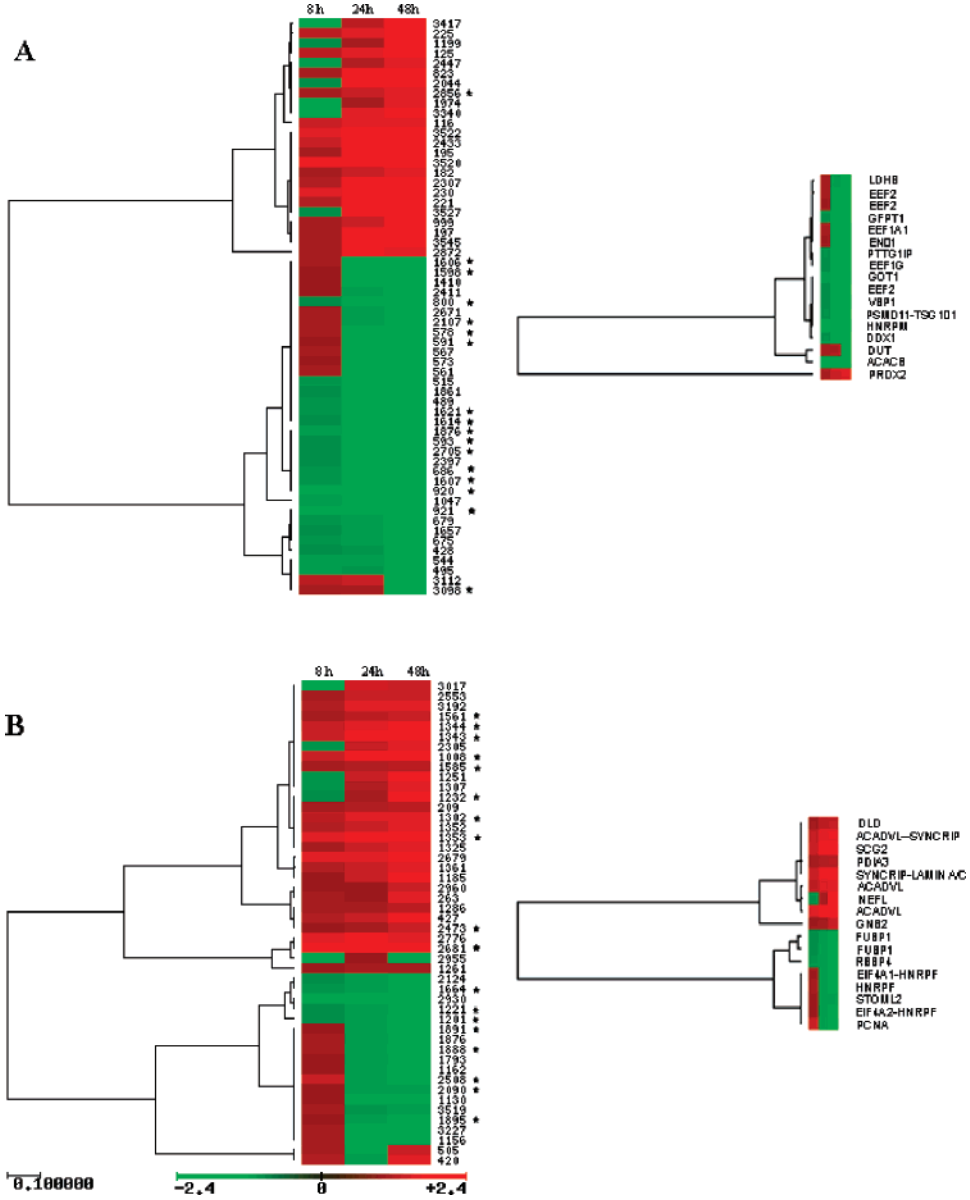

Figure 3. Hierarchical clustering analysis of protein-spots expression profiles in the cytosol (A) and nucleus (B) of the Lan5 cell line following 8, 24, and 48 h of RA treatment (by column, as indicated). The up-regulated proteins are in red; the down-regulated proteins are in green. The expression profiles of the identified protein spots, indicated by asterisks, are shown on the right side of the Figure.

phase capillary column (75 μm × 20 mm) at a flow rate of 280 nL/min and fractionated using a linear gradient of running buffer B (0.2% formic acid in 95% acetonitrile) in running buffer A (0.2% formic acid in 5% acetonitrile) from 7% to 60% in 50 min. The mass spectrometer was set up in the data-dependent MS/MS mode to alternatively acquire a full scan (m/z acquisition range from 400 to 1600 Da/e) and a tandem mass spectrum (m/z acquisition range from 100 to 2000 Da/e). The three most intense peaks in any full scan were selected as precursor ions and fragmented by collision energy. Raw MS and MS/MS spectra were elaborated by the ProteinLynx software, provided by the manufacturers that generated a peak list containing all of the fragmentation data that was used for database searching using the MASCOT MS/MS ion search software for protein identification. The list of matched peptides is reported in Table 4.

3. Protein Identification by Bionformatic Tools. Raw data from nanoLC−ESI−MS/MS analyses were converted into a Mascot format text to identify proteins by means of a Mascot software version 2.1 in home, MatrixScience.[30] The protein search both from nanoLC−ESI−MS/MS and MALDI MS analyses was governed by the following parameters: nonredundant protein sequence data base (NCBInr −20061017 database with 4 051 787 sequences and 1 396 484 404 residues downloaded; Sprot- 50.9 database with 235 673 sequences and 86 495 188 residues downloaded); specificity of the proteolytic enzyme used for hydrolysis (trypsin); taxonomic category of the sample (*Homo sapiens*); no protein molecular weight was considered; up to 1 missed cleavage; cysteines as *S*-carbamidomethylcysteines; unmodified N- and C-terminal ends; methionines both unmodified and oxidized; putative pyroGlu formation by Gln; precursor peptide maximum mass tolerance of 150 ppm and a maximum fragment mass tolerance of 100 ppm.

Data Mining. Hierarchical cluster analysis was performed using a tool available on the Internet (http://gepas.bioinfo.cnio.es/). The distance between protein expression profiles was

Table 2. Proteins Identified in the Cytosolic Fraction

master number[a]	protein name	ID NCBI	ID SPROT	theor. MW (kDa)	experim. MW (kDa)[b]	theor. p*I*	experim. p*I*[b]	MS score	MS match	fold 48/0 h	*P*-value
	Catalytic Activity (Transaminase Activity)										
800*	Glucosamine−fructose-6-phosphate aminotransferase 1	gi/183082	Q06210	77,5	-	6,39	-	166	10	-1,34	0,00014
1876	Aspartate aminotransferase, cytoplasmic	gi/105387	P17174	46,35	-	6,81	-	188	14	-1,87	0,03
	Nucleic Acid Binding (DNA Binding)										
1607*	Tumor susceptibility gene 101	gi/60655269	Q99816	44,1	-	6,06	-	276	12	-1,52	0,023
1598	Enolase 1 Variant	gi/62896593	P06733	47,5	-	7,01	-	125	12	-1,6	0,03
	Magnesium Ion Binding										
3098	dUTP pyrophosphatase	gi/181844	P33316	15,5	-	6,13	-	126	8	-1,52	0,036
	Nucleic Acid Binding (RNA Binding)										
686	DEAD box protein 1, DDX1 protein	gi/33877837	Q92499	78,8	-	8,27	-	151	17	-1,52	0,046
920	Heterogeneous nuclear ribonucleoprotein M	gi/187281	P52272	77,9	-	8,99	-	115	16	-1,78	0,021
	Protein Binding										
2705	Prefoldin subunit 3	gi/48429043	P61758	18,5	-	6,63	-	94	8	-1,73	0,0097
	Catalytic Activity (Hydrolase Activity)										
1607*	Proliferation-associated protein 2G4	gi/5453842	Q9UQ80	44,2	-	6,13	-	261	13	-1,52	0,023
	Catalytic Activity (Oxidoreductase Activity)										
2856	Peroxiredoxin-2	gi/1617118	P32119	18,5	-	5,19	-	109	8	1,51	0,078
2107	L-lactate dehydrogenase B chain	gi/49259212	P07195	36,8	-	5,86	-	184	14	-1,39	0,035
	Translation Elongation Factor Activity										
591	Human Elongation Factor 2	gi/31108	P13639	96,3	88,4	6,41	7,37	94	11	-1,56	0,014
593					88,3		7,52			-1,53	0,0036
578					88,8		7,65			-1,55	0,00017
1621	Elongation factor 1-gamma	gi/15530265	P26641	50,5	50,3	6,25	6,65	202	12	-1,73	0,018
1614					50,4		6,95			-1,69	0,022
1606*	Elongation factor 1, alpha 1	gi/48734733	P68104	50,5	-	9,14	-	241	18	-1,69	0,031
921	acetyl-CoA carboxylase beta	gi/1399290	O00763	89,8	-	6,01	-	80	14	-1,55	0,037
	Catalytic Activity (Ligase Activity)										
1607*	26S proteasome non-ATPase regulatory subunit 11	gi/2150046	O00231	47,7	-	6,08	-	318	20	-1,52	0,023
	Molecular Function Unknown										
1621	Pituitary tumor-transforming gene protein-binding factor	gi/21411022	P53801	21,2	-	9,14	-	202	5	-1,73	0,018

[a] The asterisk (*) indicates the spots that were identified by LC−MS/MS analysis. [b] Experimental MW and p*I*, calculated by DeCyder 5.0 software are reported only for proteins identified in more than one spot, in order to assess post-translational modifications.

calculated using Correlation Coefficient (linear), and the UPGMA algorithm was used to construct dendrograms.[35,36]

The proteins were classified according to the DAVID 2.1 beta annotation system (http://david.niaid.nih.gov/david/ease.htm). This tool adopts the Fisher exact test to measure the protein-enrichment in annotation terms. A Fisher exact test $P = 0$ represents perfect enrichment. If the *P*-value is equal to or smaller than 0.05, a protein would be considered strongly enriched in the annotation categories.

Western Blotting. Cells were washed three times with ice-cold PBS and scraped into extraction buffer (50 mM Tris-HCl, pH 7.5, 150 mM NaCl, 1% (v/v) Triton X-100, 10% (v/v) glycerol, and complete protease inhibitor cocktail (Roche)), transferred to 1.5 mL microcentrifuge tubes, vortexed for 15 min at 4 °C, and centrifuged at 16 100*g* for 30 min at 4 °C.

Proteins extract concentrations were determined by the Bradford assay (Bio-Rad). Thirty micrograms of total protein lysates was diluted 1:1 with Laemmli SDS-PAGE sample buffer, loaded onto 12% polyacrylamide gels, and blotted onto polyvinylidene difluoride membranes (PVDF; Bio-Rad). Membranes were blocked with 5% non-fat milk (Bio-Rad) in PBS, pH 7.6, and 0.2% Tween-20 (PBS-T), and then incubated with specific commercial goat anti-PRX II (peroxyredoxin-2), SgII (secretogranin II), NF-L (68 kDa neurofilament), EF-2 (elongation factor-2), prefoldin subunit 3 and Gβ2 (guanine-nucleotide-binding protein beta subunit 2) antibodies, a mouse anti-PCNA (proliferating cell nuclear antigen) antibody (1:100) (Santa Cruz Biotechnology, Santa Cruz, CA), and a rabbit anti-EF1α (eukaryotic elongation factor) antibody (1:100) (Upstate) at 4 °C overnight.

After a washing step in PBS-T, the membranes were incubated with a horseradish peroxidase (HRP)-conjugated anti-goat, anti-mouse, anti-rabbit antibody (1:10 000) (Santa Cruz Biotechnology), and the immunoblots were visualized using ECL detection kits, with enhanced chemiluminescence (Pierce). A mouse β-actin antibody (1:1000) (Santa Cruz Biotechnology, Santa Cruz, CA) was used as the control for equal loading. The protein bands images on X-ray films were acquired with the GelDoc 2000 system (Bio-Rad). The densitometric measurements were performed by Quantity One 4.5 tool (Bio-Rad).

Results

DIGE Analysis of Differentially Expressed Proteins Following ATRA Treatment in the LAN-5 NB Cell Line. To determine the molecular mechanisms involved in ATRA-induced differentiation in NB, we examined changes in the proteome of LAN-5 NB cells. We analyzed the proteome in two different cellular fractions, enriched in either cytosolic or nuclear proteins. We checked the quality of these fractions by Western blotting using specific markers (Figure 1). The biochemical protein markers for nuclei included lamin β (LMβ), a marker of structural components of the nuclear matrix, and the transcriptional factor SP1, a marker of the soluble nuclear fraction. As Figure 1 shows, LMβ and SP1 were mostly detected in the nuclear fraction; on the contrary, the cytosolic biochemical protein marker enolase (ENO) is mostly present in the cytosolic fraction, and only seen at low levels in the nuclear extract (Figure 1A). Moreover, we checked the enrichment of some organelles in both fractions. We used cytochrome P450 reductase as a marker of mitochondria and lysosome-associated membrane glycoprotein 2 (LAMP-2) as a marker of lysosomes. We observed that the nuclear fraction was also enriched in these organelles (Figure 1B).

The differential expression of the LAN-5 cytosolic and nuclear proteins as a function of ATRA treatment was analyzed at 8, 24, and 48 h of ATRA treatment using DIGE in a pH range

Table 3. Proteins Identified in the Nuclear Fraction

master number[a]	protein name	ID NCBI	ID SPROT	theor. MW (kDa)	experim. MW (kDa)[b]	theor. p*I*	experim. p*I*[b]	MS score	MS match	fold 48/0 h	*P*-value
			Nucleic Acid Binding (RNA Binding)								
1895	Heterogeneous nuclear ribonucleoprotein F	gi/76780063	P52597	46	45,7	5,38	5,04	103	9	-1,27	0,0037
1888					45,8		5,12			-1,35	0,014
1891					45,7		5,17			-1,44	0,0000072
1891	Eukaryotic initiation factor 4A-I	gi/77735407	P60842	46	-	5,38	-	186	7	-1,44	0,0000072
1895	Eukaryotic initiation factor 4A-II	gi/16198386	Q14240	46,6	-	5,38	-	256	11	-1,27	0,0037
1343*	Heterogeneous nuclear ribonucleoprotein Q	gi/21619168	O60506	58,95	58,3	7,18	6,52	325	7	1,68	0,02
1302*					58,8		6,68			1,59	0,00029
1353*					58,5		6,87			1,87	0,0055
1344+*					58,6		7,06			1,65	0,00035
			Structural Constituent of Cytoskeleton								
1232	68 kDa neurofilament protein	gi/24658018	P07196	61,6	-	4,64	-	111	8	2,12	0,0018
			Nucleic Acid Binding (DNA Binding)								
1201	FUSE-binding protein 1	gi/37078490	Q96AE4	67,65	62,1	7,18	6,43	178	13	-1,29	0,013
1221					62		6,7			-1,26	0,0099
2508	Proliferating cell nuclear antigen	gi/2914387	P12004	29,1	-	4,57	-	115	8	-1,75	0,003
			Structural Molecule Activity								
1343*	lamin A/C	gi/55957499	P02545	69,5	-	6,4	-	386	7	1,68	0,02
			Nucleotide Binding								
1561	Dihydrolipoyl dehydrogenase, mitochondrial	gi/71042410	P09622	50,7	-	6,35	-	86	7	-1,38	0,037
			Protein Binding								
1664	Histone-binding protein RBBP4	gi/30583457	Q09028	47,95	-	4,74	-	149	10	-1,38	0,0037
			Metal Ion Binding								
1008	SecretograninII, Chromogranin C	gi/134464	P13521	70,85	-	4,67	-	83	8	3,13	0,00032
			Signal Transducer Activity								
2473	Guanine nucleotide-binding protein beta subunit 2	gi/20357529	P62879	38,1	-	5,6	-	148	11	1,44	0,01
2090	Stomatin (EPB72)-like 2	gi/14603403	Q9UJZ1	38,65	-	6,88	-	125	11	-1,21	0,054
			Catalytic Activity (Hydrolase Activity)								
1585	Disulfide isomerase ER-60	gi/860986	P30101	57,1	-	6,1	-	118	13	1,23	0,0027
			Catalytic Activity (Oxidoreductase)								
1353*	Very long chain acyl CoA dehydrogenase	gi/3273228	P49748	70,85	58,5	8,88	6,87	600	10	1,87	0,0055
1302*					58,8		6,68			1,59	0,00029
1344*					58,6		7,06			1,65	0,00035
2681	brain and muscle Ah receptor nuclear translocator-like protein	gi/7512308		31,6	-	9,42	-	94	7	2,14	0,041

[a] The asterisk (*) indicates the protein spots that were identified by LC−MS/MS. [b] Experimental MW and p*I*, calculated by DeCyder 5.0 software are reported only for proteins identified in more than one spot, in order to assess post-translational modifications.

of 3.0−10.0. The samples were labeled according to the scheme shown in Table 1. To increase biological and statistical significance of the results, we prepared the protein lysates from three independent treatments of LAN-5 NB cultures. Accordingly, each experiment required two sets of gels (see Table 1).

The protein extracts to compare were prelabeled with either Cy3 or Cy5 fluorescent dyes. Each Cy3/Cy5-labeled sample pair was co-mixed with a Cy2-labeled pooled standard sample containing an equal amount of all 12 samples analyzed both for cytosolic and nuclear fractions. The Cy2/Cy3/Cy5 labeled samples run together on the same gel. Furthermore, we interchanged the labeling design in the third experiment to reduce the effects of preferential binding of dyes to proteins. For each gel, the Cy3, Cy5, and Cy2 images were imported into the DeCyder DIA (difference in-gel analysis) module to reveal the differentially expressed protein spots featured in each gel. To identify the differentially expressed protein spots across the six gels, both for cytosolic and nuclear fractions, the results from the intra-gel comparison (six DIA files) were imported into the BVA module of DeCyder Software. For the cytosolic and nuclear fractions, one Cy2 image was selected as the master image, and the other five internal standard images were matched sequentially to it (Figure 2).

Approximately, 3000 protein spots were detected for both the cytosolic and the nuclear fractions. The protein spots were then filtered for the statistically relevant trend of regulation ($p \leq 0.075$; Student's paired t test) among the various ATRA treatment time points used. The analysis allowed us to find 126 statistically relevant and differentially expressed spots: 58 from the cytosolic fraction, and 68 from the nuclear fraction, with fold changes >1.3 or ≤1.3 (48 vs 0 h). In particular, 24 spots were more highly expressed and 34 spots were less expressed in the cytosolic fractions, with 43 spots and 25 in the nuclear fractions, respectively.

The RA-induced proteome changes were classified on the basis of the expression profiles of these 126 protein spots using hierarchical clustering. As shown in Figure 3, the DeCyder analysis data from both the cytosolic and nuclear fractions divide along two main branches, with each dividing further into two branches, showing evidence of four major categories: two up-regulated categories in the upper dendrogram, and two down-regulated categories in the lower dendrogram. We observed that in the two cellular compartments there are two subclusters denoting proteins highly expressed at the 8 h and then lower expressed at 48 h, and proteins that are lower expressed at 8 h and then highly expressed at 48 h.

To identify the differentially expressed proteins, 38 spots of interest were excised from the preparative gels, and in-gel trypsin digestion and mass spectrometry (MS/MS) analysis were performed for protein identification. Successful identification was achieved if at least five peptides of experimental MS/MS data matched the internal sequence of the theoretical candidate protein. Mass spectrometric analysis identified 33 proteins corresponding to 17 protein spots from the cytosolic fraction, and 16 from the nuclear fraction. The results of the protein identification are given in Tables 2 and 3, and the positions of the differentially expressed spots picked in the 2D gel are shown in Figure 4.

In this study, we were not able to determine the identities of the protein components of other differentially expressed spots using either the MALDI-TOF or LC−MS/MS mass spectrometric techniques. This may in part be due to insufficient

Table 4. LC−MSMS Matched Peptides

spot	protein name	coverage	start-end	matched peptides
	Proteins Identified in the Cytosolic Fraction			
800	glutamine:fructose-6-phosphate amidotransferase	13%	164−176	esqdtsfttlver
			191−202	svhfpgqavgtr
			203−212	rgsplligvr
			204−212	gsplligvr
			217−227	lstdhipilyr
			319−327	gnfssfmqk
			512−518	rlpdlik
			519−529	evlsmddeiqk
			602−612	cqnalqqvvar
			665−672	gydvdfpr
1606	Eukaryotic translation elongation factor 1 alpha 1	34%	6−20	thinivvighvdsgk
			21−30	stttghliyk
			38−51	tiekfekeaaemgk
			85−96	yyvtiidapghr
			135−146	ehallaytlgvk
			147−154	ytlgvkqlivgvnk
			166−172	ryeeivk
			167−179	yeeivkevstyik
			173−180	evstyikk
			256−266	iggigtvpvgr
			267−290	vetgvlkpgmvvtfapvnvttevk
			396−423	sgdaaivdmvpgkpmcvesfsdypplgr
			428−439	dmrqtvavgvik
			431−439	qtvavgvik
1607	26S proteasome subunit 9	40%	12−20	aqsllstdr
			47−59	eqsilelgslak
			60−71	tgqaaelgglk
			72−82	yvrpflnsisk
			133−142	lvslyfdtkr
			143−155	yqealhlgsqllr
			176−185	llesktyhalsnlpk
			253−258	ymllck
			259−274	imlntpedvqalvsgk
			298−304	aqasknrsladfek
			311−325	aelrddpiisthlak
			315−325	ddpiisthlak
			326−337	lydnlleqnlir
			338−344	viepfsr
			345−355	vqiehisslik
			365−373	lsqmildkk
			410−417	vvdslynk
1607	tumor susceptibility gene 101	28%	2−9	avsesqlk
			34−50	dlkpvldsyvfndgssr
			51−64	elmnltgtipvpyr
			218−227	dgtisedtir
			228−237	aslisavsdk
			242−248	mkeemdr
			249−258	aqaelnalkr
			270−276	leemvtr
			293−304	kkdeelssalek
			369−374	kqfqlr
			382−390	ktaglsdly
1607	proliferation-associated 2G4	28%	23−30	mggdianr
			200−210	tiiqnptdqqk
			264−271	affsever
			272−281	rfdampftlr
			273−281	fdampftlr
			291−298	mgvvecak
			299−311	hellqpfnvlyek
			312−320	egefvaqfk
			321−332	ftvllmpngpmr
			333−344	itsgpfepdlyk
			345−355	semevqdaelk
			356−364	allqssasr
	Proteins Identified in the Nuclear Fraction			
1302	very-long-chain acyl-CoA dehydrogenase	19%	205−229	lasgetvaafcltepssgsdaasir
			279−286	itafvver
			304−316	asntaevffdgvr
1302	very-long-chain acyl-CoA dehydrogenase	19%	317−331	vpsenvlgevgsgfk
			342−353	fgmaaalagtmr
			420−428	ifgseaawk
			460−469	ifegtndilr
			483−492	elsglgsalk
			493−507	npfgnaglllgeagk
			539−550	aleqfatvveak

Table 4 (Continued)

spot	protein name	coverage	start-end	matched peptides
	Proteins Identified in the Nuclear Fraction			
1302	hnRNP Q	28%	39−60	vaekldeiyvaglvahsdlder
			92−100	saflcgvmk
			144−168	yggpppdsvysgqqpsvgteifvgk
			172−184	rdlfedelvplfek
			185−192	agpiwdlr
			193−203	lmmdpltglnr
			204−213	gyafvtfctk
			255−265	tkeqileefsk
			257−265	eqileefsk
			266−282	vtegltdvilyhqpddk
			287−297	gfcfleyedhk
			309−321	nlantvteeilek
1343	hnRNP Q	8%	185−192	agpiwdlr
			257−265	eqileefsk
			193−203	lmmdpltglnr
			131−142	tgytldvttgqr
			255−265	tkeqileefsk
			344−356	derdgavkameem
1343	lamin A/C	11%	209−216	niyseelr
			241−249	ladalqelr
			145−155	eaalstalsek
			79−89	aayeaelgdar
			320−329	lrdledslar
			528−541	alinstgeevamr
			281−296	nsnlvgaaheelqqsr
1344	very-long-chain acyl-CoA dehydrogenase	27%	1−12	mqaarmaasl gr
			72−79	sfavgmfk
			112−121	ffeevndpak
			279−286	tafvver
			317−331	vpsenvlgevgsgf k
			342−353	fgmaaalagtmr
			420−428	ifgseaawk
			460−469	ifegtndilr
			470−480	lfvalqgcmdk
			481−492	gkelsglgsalk
			483−492	elsglgsalk
			493−507	npfgnaglllgeagk
			513−531	aglgsglslsglvhpelsrsg
			539−550	leqfatvveak
			557−567	givneqfllqr
			616−632	egmaalqsdpwqqelyr
1344	hnRNP Q	9%	131−142	tgytldvttgqr
			185−192	agpiwdlr
			204−213	lnrgyafvtfctk
			255−265	tkeqileefsk
			309−321	nlantvteeilek
1353	very-long-chain acyl-CoA dehydrogenase	24%	265−278	tpvtdpatgavkek
			279−286	itafvver
			304−316	asntaevffdgvr
			317−331	vpsenvlgevgsgf k
			342−353	fgmaaalagtmr
			420−428	ifgseaawk
			460−469	ifegtndilr
			470−480	lfvalqgcmdk
			481−492	gkelsglgsalk
			483−492	elsglgsalk
			493−507	npfgnaglllgeagk
			513−531	aglgsglslsglvhpelsr
			539−550	aleqfatvveak
			645−655	tvveaklikhk
1353	hnRNP Q	14%	131−142	tgytldvttgqr
			172−184	dlfedelvplfek
			185−192	agpiwdlr
			204−213	gyafvtfctk
			255−265	tkeqileefsk
			287−297	gfcfleyedhk
			309−321	nlantvteeilek

amounts of protein in the spots, and also to the scarcity of tryptic digestion sites. In several cases, some well-separated spots of similar mass but different charge were identified as the same proteins. This may imply alternative post-translational modifications, such as phosphorylation or multiple expression forms. These possibilities have not been studied further to date. Similarly, some different proteins comigrated in the same spot under our experimental conditions, and the identified pituitary

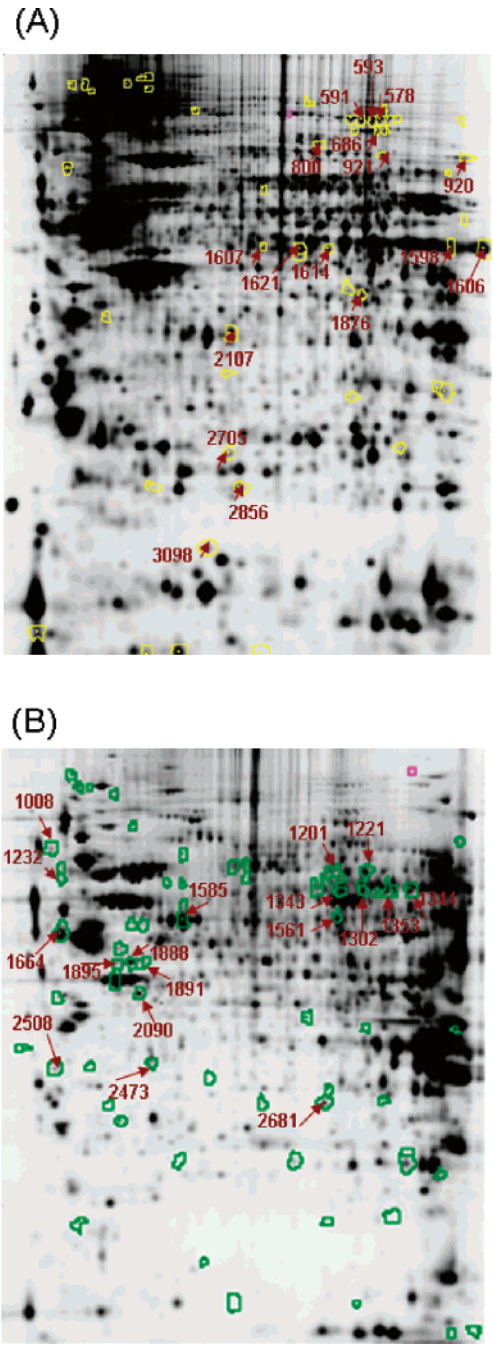

Figure 4. The differentially expressed protein spots upon ATRA treatment, for cytosolic (A; 58) and nuclear fractions (B; 68). The arrows show the picked-up spots on the preparative gels and then identified: 17 spots for the cytosolic fraction and 16 spots for the nuclear fraction.

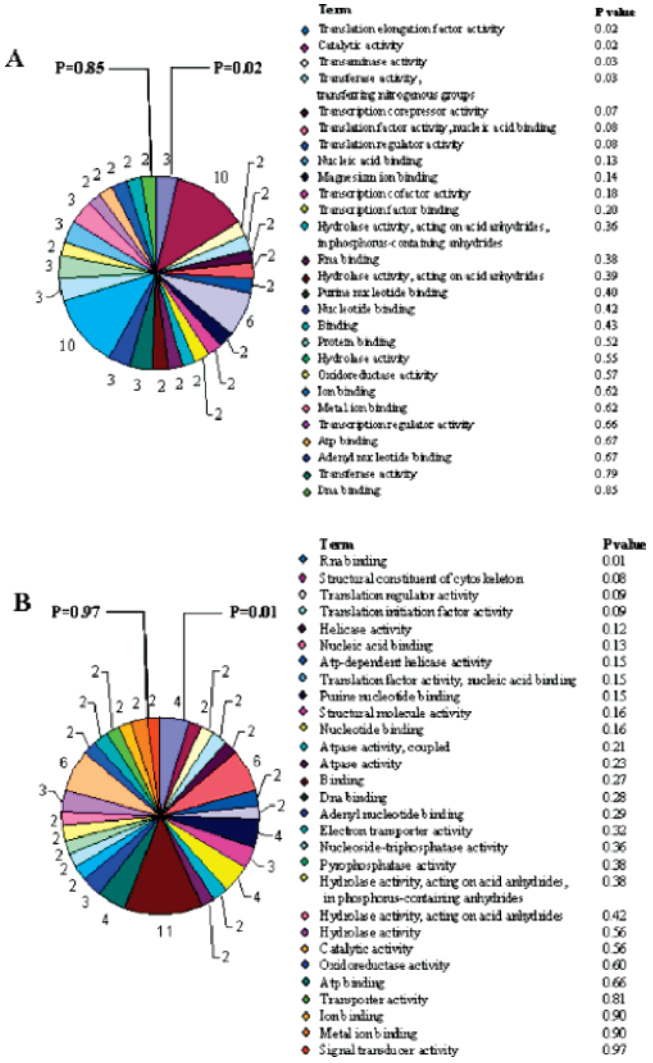

Figure 5. The proteins identified were classified using the DAVID 2.1 beta annotation system. The Fisher exact test was used to determine the protein-enrichment in annotation terms. The functional categories are sorted by *P*-value. Statistical analyses (Fisher exact test) of the cytosol proteins (A) and the nuclear proteins (B) are shown. The graphic shows the number of proteins within each functional category.

tumor-transforming gene protein-binding factor PTTG1IP was detected in a spot which differed from its theoretical molecular mass and p*I*. This could reflect proteolytic degradation of the protein or post-translational modifications, such as glycosylation.

We performed functional classification of the proteins identified according to the DAVID 2.1 beta annotation system. Statistical analysis (Fisher exact test) of the 17 cytosolic proteins identified (Figure 5A) indicated that some functional categories are overrepresented in this list, such as translation elongation factor activity, catalytic activity, transaminase activity, transferase activity, and the transferring of nitrogenous groups. Moreover, the functional category RNA binding was overrepresented in the list of the 16 nuclear proteins identified (Figure 5B).

To examine the correlations between the proteins showing RA-induced differential expression and the chromosomal rearrangements or epigenetic regulatory loci in NB, we searched for the physical location of the genes coding for the differentially expressed proteins, using UNIGENE searching of the NCBI genome database. This revealed that the DLD (dihydrolipoamide dehydrogenase), ENO1 (enolase variant 1), DDX1 (ATP-dependent RNA helicase), ACACB (acetyl-CoA carboxylase beta), PSMD11 (26S proteasome non-ATPase regulatory subunit 11) genes map to allelic imbalance chromosomal regions involved in NB (Table 5).

Validation and Analysis in Different Human NB Cell Lines. We performed validation of the data for some of the identified proteins based on the availability of good commercial antibody by Western blotting: PRX II (peroxyredoxin-2), SgII (secretog-

Table 5. Mapped Chromosomal Regions of Genes Coding for the Identified Proteins

protein name	gene name	mapped chromosomal regions[a]
Glucosamine-fructose-6-phosphate aminotransferase 1	GFPT1	2p13
Aspartate aminotransferase, cytoplasmic	GOT1	10q24.1−25.1
Tumor susceptibility gene 101	TSG101	11p15
Enolase 1 Variant	ENO1	1p36.3−p36.2*
dUTP pyrophosphatase	DUT	15q15−21.1
DEAD box protein 1, DDX1 protein	DDX1	2p24*
Heterogeneous nuclear ribonucleoprotein M	HNRPM	19p13.3−p13.2
Prefoldin subunit 3	VBP1	Xq28
Proliferation-associated protein 2G4	PA2G4	12q13
Peroxiredoxin-2	PRDX2	19p13.2
L-lactate dehydrogenase B chain	LDHB	12p12.2−p12.1
Human Elongation Factor 2	EEF2	19pter−q12
Elongation Factor 1-gamma	EEF1G	11q12.3
Elongation Factor 1, alpha 1	EEF1A1	6q14.1
acetyl-CoA carboxylase beta	ACACB	12q24.11*
26S proteasome non-ATPase regulatory subunit 11	PSMD11	17q11.2*
Pituitary tumor-transforming gene protein-binding factor	PTTG1IP	21q22.3
Heterogeneous nuclear ribonucleoprotein F	HNRPF	10q11.21−11.22
Eukaryotic initiation factor 4A-I	EIF4A1	17p13
Eukaryotic initiation factor 4A-II	EIF4A2	3q28
Heterogeneous nuclear ribonucleoprotein Q	SYNCRIP	6q14−15
68 kDa neurofilament protein	NEFL	8p21
FUSE-binding protein 1	FUBP1	1p31.1
Proliferating cell nuclear antigen	PCNA	20pter−p12
lamin A/C	LMNA	1q21.2−21.3
Dihydrolipoyl dehydrogenase, mitochondrial	DLD	7q31−32*
Histone-binding protein RBBP4	RBBP4	1p35.1
SecretograninII, Chromogranin C	SCG2	2q35−36
Guanine nucleotide-binding protein beta subunit 2	GNB2	7q21.3−22.1
Stomatin (EPB72)- like 2	STOML2	9p13,1
Disulfide isomerase ER-60	PDIA3	15q15
Very long chain acyl CoA dehydrogenase	ACADVL	17p13−p11
brain and muscle Ah receptor nuclear translocator-like protein	§	§

[a] Asterisk (*) denotes genes coding for the identified proteins that are mapped to regions known to be altered in NB.

ranin II), NEF-L (68kDa neurofilament), eEF-1α (eukaryotic elongation factor), PCNA (proliferating cell nuclear antigen), EF-2 (elongation factor-2), prefoldin subunit 3 and Gβ2 (guanine-nucleotide-binding protein beta subunit 2) (Figure 6A). Semi-quantitative analysis of the protein expression was performed at the four time points of the differentiation: 0, 8, 24, and 48 h. The bands were quantified by densitometry to obtain an integral optic density (IOD) value which then was normalized with respect to β-actin value (Figure 6B). All of these proteins showed differential expression patterns in the LAN-5 cell line, according to the DIGE results. We also analyzed the expression patterns of these selected proteins in two other NB cell lines, SH-SY5Y and SK-N-BE, not treated and treated with RA for 48 h (Figure 7A). Here, the proteins TSA, SgII, NF-L, EF1α, PCNA, and EF-2 showed the same trends seen in the LAN-5 cells, while the prefoldin 3 and Gβ2 proteins were differentially expressed in the SH-SY5Y cells, and not in the SK-N-BE cells. Semiquantitative analysis of the protein expression at the two extreme time points of differentiation: 0 and 48 h, in LAN-5, SH-SY-5Y, and SK-N-BE cells was shown in Figure 7B.

Discussion

NB shows the highest rate of spontaneous regression of any human tumor, mainly due to differentiation and maturation of these highly malignant cells in neurons. It is of interest to study the molecular pathways driving spontaneous regression in NB to unravel the molecular basis of NB development and to determine the differentiation therapies that can be used to treat patients.

ATRA, the most commonly used anti-neoplastic agent in NB therapy, can induce neural differentiation in NB cell lines *in vitro*.[4] Systematic approaches at the transcriptional and translational levels have been used to identify the target genes for NB progression. Moreover, studies of differentiation induced by ATRA have been performed in PML cells and in mouse stem cells using a proteomic approach.

The main aim of our study was to gather insight into the molecular mechanisms of NB differentiation using 2-D DIGE technology. We used the human LAN-5 NB cell line amplified for the oncogene N-MYC and responsive to ATRA treatment,[37,38] and monitored the cytosolic and nuclear protein expression in those cells at the early phase of ATRA differentiation. We used 5 μM ATRA, according to the known pharmacological doses used in phase I trials of RA administrated to NB patients.[39]

We detected a total of 58 spots in the cytosolic fraction and 68 in the nuclear fraction that showed differences in their relative expression between the control and RA-treated LAN-5 cells; 33 of these proteins were identified (17 in the cytosolic fraction and 16 in the nuclear fraction). In agreement with the neuronal-orientated differentiation induced by ATRA, we observed at early phase of differentiation a substantial up-regulation of the NEF-L and SgII proteins, which are known to be neuronal markers,[40−42] and the down-regulation of the proliferating cell nuclear antigen PCNA, an auxiliary protein of DNA polymerase. The highest levels of PCNA were seen in advanced NB stage tumors with an amplified N-myc gene.[43,44] Our results suggest that the decreased levels of PCNA may

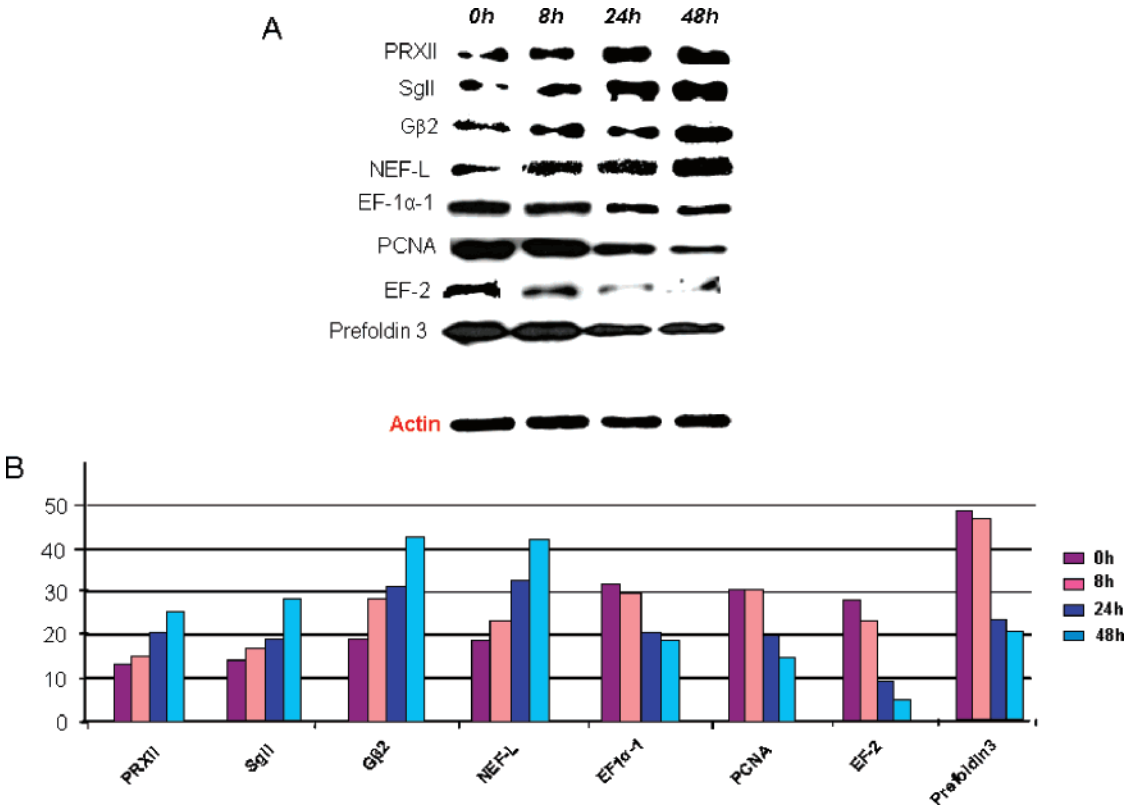

Figure 6. Western blot analysis of selected proteins was performed in LAN-5 cells, not treated or treated with 5 μM RA for 8, 24, and 48 h. The β-actin was used as the loading control (A). The bands were quantified by densitometry. The bar graph shows integral optic density (IOD) value for each band, normalized with respect to β-actin expression (B).

reflect differences in proliferative activity and that the suppression of proliferation is an obligatory step in the differentiation of these cancer cells. Furthermore, we saw that Far upstream element Binding Protein 1 (FBP) was down-regulated upon differentiation. FBP stimulates the expression of c-myc, a transcription factor involved in cell growth, proliferation, differentiation, and apoptosis.[45] Low expression of FBP has also been seen in differentiated haematopoietic stem cells.[46]

Closed examination of the identified differentially expressed proteins shows that those of greatest relevance are annotated to the "translational elongation factor activity" and "RNA-binding" functional categories. Most of the proteins related to these categories were down-regulated during RA differentiation. Among these, the initiation factor IF-2, the elongation factors eEF-1gamma and eEF-1alpha1, the heterogeneous nuclear ribonucleoprotein hnRNP F, and the eukaryotic initiation factors eIF4A-1 and eIF4A-2 are known to be down-regulated by ATRA in acute promyelocytic cells.[27−29] In particular, IF-2, eEF-1gamma and eEF-1alpha1 have roles in the elongation stages of the protein synthesis mechanism, and hnRNP F, eIF4A-1 and eIF4A-2 have roles in mRNA processing and transport. This may suggest that ATRA-induced differentiation of NB could share these six effectors with ATRA-induced differentiation in PML cells.

A group of enzymes involved in biochemical metabolism was found to be significantly down-regulated, implicating the suppression of related biochemical pathways in ATRA-treated cells (dihydrolipoyl dehydrogenase, glucosamine-fructose-6-phosphate aminotransferase 1, aspartate aminotransferase, enolase variant 1, L-lactate dehydrogenase B chain, acetyl CoA carboxylase beta). The down-regulation of lactate dehydrogenase (LDH) is also interesting, as it is a characteristic serum marker that is useful in facilitating diagnosis, prognosis, and monitoring disease progression in children affected by NB.

Several genomic alterations in NB have been reported to correlate with prognosis, including amplification of MYCN oncogene, gain of chromosome 17q and loss of chromosome 1p36. Other recurrent changes have also been suggested to have relevance to the development and progression of these tumors.[47,48] Our results show that some of the genes coding for the identified proteins mapped to chromosomal regions that are known to be altered in NB. Among these are the acetyl CoA carboxylase beta ACACB gene which is mapped to allelic imbalance NB region (17p13-p11) and the ENO1 gene which is mapped into a loss chromosomal NB region (1p36.3-1p36.2)[49,50] Moreover, enolase variant 1, which was down-regulated in our system, has been seen to be up regulated in undifferentiated haematopoietic cells.[46] The DLD, DDX1, and PSMD11 genes mapped to gain NB regions[50−52] The dihydrolipoyl dehydrogenase DLD protein level, which is down-regulated in our model system, has been seen to increase in the central nervous system of rats after oxidative stress.[53] The DDX1 gene coding for the DEAD box protein 1, which is down-regulated in our model system, has been shown to be overexpressed in a subset of unfavorable NBs and in retinoblastoma cell lines;[54] it has been mapped to chromosome 2p24 and found often co-amplified with the proto-oncogene MYCN in patients with a worse prognosis[55,56] than in patients with only the MYCN gene amplified.[57,58] The role of DDX1 in the tumorigenic process is not known though; it is a putative RNA helicase, predicted to be involved in RNA binding and in the export of mRNA from the nucleus to the cytoplasm.[59,60] It is both cytoplasmatic and

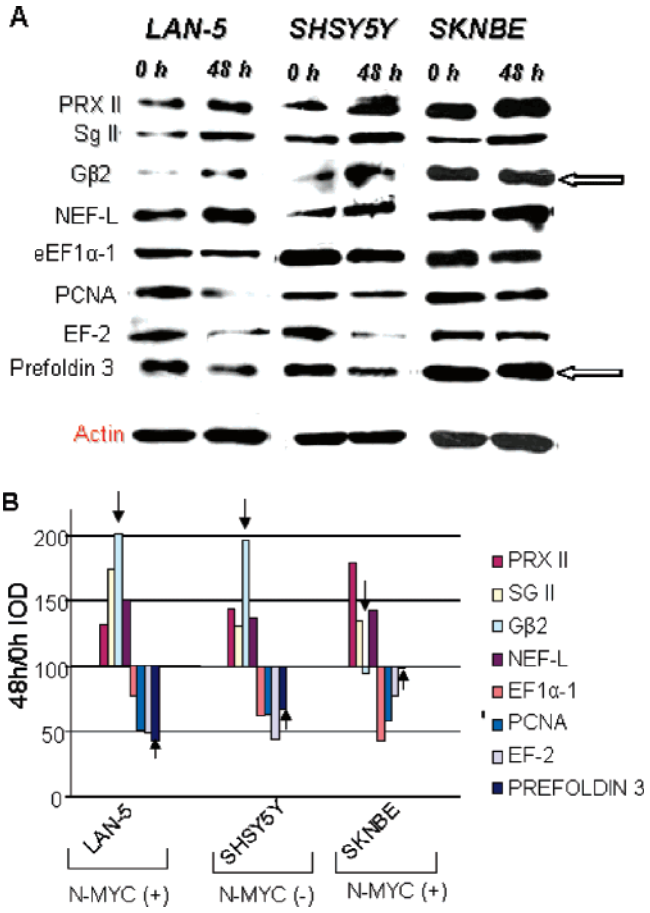

Figure 7. Western blot analysis of selected proteins was performed in LAN-5, SH-SY5Y and SK-N-BE cells, with (+) and without (-) N-MYC amplification, either not treated or treated with 5 μM RA for 48 h. The β-actin was used as the loading control (A). The bands were quantified by densitometry to obtain an integral optic density (IOD) value which then was normalized with respect to their β-actin expression value. The bar graph shows the fold of induction at 48 h of RA differentiation in the three NB cell lines. The fold was expressed as percentage; proteins expression level at 0 h was assigned equal to 100% (B). The arrows show two proteins which were found differentially expressed in LAN-5 and SH-SY5Y cells and not differentially expressed in SK-N-BE cells.

nuclear in DDX1-MYCN amplified NB and RB cell lines. However, it is known to localize specifically to the nucleus in non MYCN amplified cell lines. In LAN-5 cells, we observed a correlation between MYCN amplification and DDX1 nuclear translocation upon ATRA treatment. These findings may support the hypothesis of its putative RNA shuttle function into the nucleus as a sign of good prognosis upon ATRA differentiation (Figure. 1S in Supporting Information).

Other down-regulated proteins identified in our study have been associated with the aggressiveness of several tumors. This would suggest that the cells are regressing from their tumoral state, following RA treatment. Among these, there are pituitary tumor-transforming gene protein-binding factor PTTG1IP and ribonucleoprotein hnRNP F. PTTG1IP is a prognostic indicator in thyroid cancer, even if its precise contribution to tumorigenesis has not yet been explored.[61] Also, increased expression of hnRNP F has been seen in more aggressive colorectal tumors. This suggests hnRNP F as a potential marker for colorectal cancer progression.[62] Furthermore, the DDX1, eIF4A1, eIF4A2, eEF1-gamma, and LDH genes are detected in several NB cDNA libraries. Moreover, eIF4A1 mRNA has been shown to be consistently overexpressed in human melanoma cells *in vitro*,[63] in hepatocellular carcinoma[64,65] and in early stage non−small-cell lung cancer.[66]

The SH-SY5Y and SK-N-BE human NB cell lines are able to undergo neuronal differentiation in the presence of ATRA. The SH-SY5Y cell line is not amplified,[67] and the SK-N-BE cell line is amplified for the oncogene MYCN,[68] an important determinant of RA response *in vitro* and patient prognosis *in vivo*.[69,70] Either has often been used as one of the models for the analysis of neuronal function and differentiation. According to it, we saw that the neural markers SgII and NEF-L and the proliferating marker PCNA were differentially regulated by RA in the SH-SY5Y and SK-N-BE cell lines as compared to the LAN-5 cell line. In the three cell lines, we also observed the PRDX2 protein up-regulation which has been seen in the SH-SY5Y cell line upon treatment with the anti-neoplastic drug ectoposide[22] and during differentiation of embryonic stem cells to neural cells by ATRA.[29] Moreover, we observed that the ATRA treatment down-regulates the EF1α and EF-2 proteins, and this effect has just been reported in promyelocitic cells.

After ATRA treatment, Gβ2 and prefoldin subunit 3 were differentially expressed in the SH-SY5Y cells as compared to the LAN-5 cells, although they were not differentially expressed in the SK-N-BE cell line. Here, we assay three independent cell lines: two N-MYC-duplicated and one without amplification. Indeed the three cell lines have different tumoral origins, and the un-regulation of these two proteins in SK-N-BE cells might suggest that NB ATRA-induced differentiation may involve different pathways. Gβ2 is an important regulator of certain signal-transduction receptors and effectors and is ubiquitously expressed in human tissues. Nothing of this protein was known to be associated with the tumor process or to be regulated by RA. Prefoldin subunit 3/vbp1 protein is a chaperone that captures proteins in unfolded state and transfers them to cytosolic chaperonin for functional folding. To our knowledge, the role of prefoldin proteins is not known in differentiation *per se* or in neural differentiation. We saw that it decreased in cytosolic fraction upon RA treatment. Through proteomic approach it was found that proteins containing prefoldin structures increased during neural differentiation.[71] Additionally, it was shown that the chaperonin prefoldin 3 binds the Von Hippel-Lindau (VHL) tumor suppressor gene product.[72,73] VHL is involved in the ubiquitination and subsequent proteasomal degradation via the VHL ubiquitination complex[74,75] and in the down-regulation of transcriptional elongation.[76] Because prefoldin 3 functions as a chaperone protein, it may play a role in the transport of the Von Hippel-Lindau protein from the perinuclear granules into the cytoplasm for the ubiquitination of hypoxia-inducible factor, an important step in the development of angiogenic tumors. VHL gene alteration leads to VHL disease which is associated with various rare neoplasias, including haemangioblastoma of the central nervous system, retinal angioma, clear cell renal carcinoma, and pheochromocytoma[77] (OMIM 193300). VHL gene is mapped on chromosome 3p25, and the loss of this region is a nonrandom alteration associated with aggressive NBs.[78] Furthermore, its mRNA expression level is a promising marker to predict patient survival in NB.[79] It is known the inhibition of endogenous expression of VHL protein in SHSY5Y cells reduced neuronal properties. In conclusion, VHL protein has a neuronal differentiating potential to transform NB cells into functional

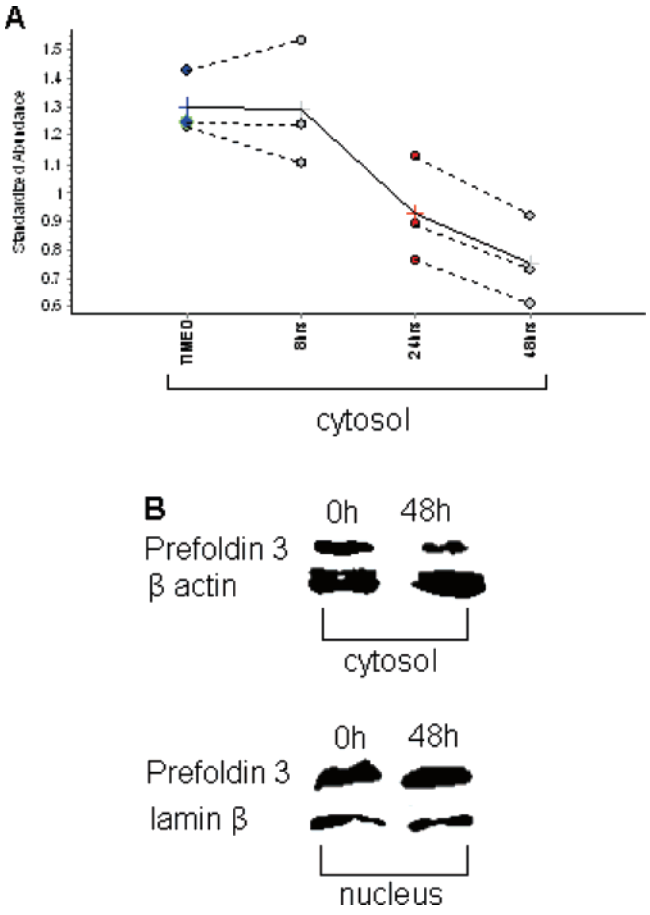

Figure 8. Prefoldin 3 DIGE differentially expression in cytosolic fraction was output by Biological Variation Analysis (BVA). Each point represents the standardized log abundance (sample/internal standard) of a protein spot obtained for each of the 12 gels analyzed: 3 gels loaded proteins at 0 h, 3 gels loaded proteins at 8 h RA, 3 gels loaded proteins at 24 h RA, and 3 gels loaded proteins at 48 h RA. A paired Student's *t* test was applied to all samples, yielding a *p*-value of 0.0097 and fold 48 h/0 h of −1.73 (A). Western blotting of prefoldin 3 was performed in cytosolic and nuclear fractions of LAN-5 cells, not treated or treated with 5 μM RA for 48 h. The β-actin and lamin β were used as the loading control in cytosolic fraction and nuclear fraction, respectively (B).

neuron-like cells.[80,81] To date, the role of prefoldin 3 in NB has not been investigated. It is known to have a cytoplasmatic location, but in the presence of VHL the protein has a nuclear location.[82] As shown in Figure 8, prefoldin 3 has a preferential location in the nuclear compartment upon ATRA differentiation, while in the cytoplasm, a decreased expression is observed. This data underline the potential new role of prefoldin 3 in the nuclear compartment during the differentiation process which could be issue of future studies on NB tumors to demonstrate the role of prefoldin 3 together with VHL protein in the progression of NB.

Conclusions

We have used the 2D-DIGE technique to analyze the proteome of the human LAN-5 NB cell line upon RA treatment. We have identified at least 33 proteins that were differentially expressed during RA treatment, and that have important roles in a variety of pathways. The RA differential expression patterns of some of the identified proteins were analyzed in other human NB cell lines. We saw that two analyzed proteins are unregulated in SK-N-BE cells as compared to LAN-5 cells. This suggests that NB ATRA-induced differentiation may involve different pathways. Additionally, we hypothesize that prefoldin 3 protein, found through these proteomic approach down-regulated into the cytoplasm during differentiation, may acts as an oncogene through the binding of VHL tumor suppressor protein in NB. In conclusion, our results provide insight toward the identification of RA-induced differentiation gene-proteins in NB, as an attempt to search for new prognostic markers.

Acknowledgment. We thank the SEMM, the European School of Molecular Medicine, Prof. Piero Pucci and his collaborators for mass spectrometry identifications, the Centro regionale di competenza GEAR, regione Campania, for 2D-DIGE facility and the financial support of (1) OPEN-Associazione Oncologia Pediatrica e Neuroblastoma-ONLUS, (2) Fondazione per la lotta al Neuroblastoma-ONLUS, and (3) l'Associazione Italiana per la Ricerca sul Cancro AIRC.

Supporting Information Available: Supplementary Figure 1 (Figure. 1S), Western blot analysis of DDX1 protein. This material is available free of charge via the Internet at http://pubs.acs.org.

References

(1) *Neuroblastoma*; Brodeur, G. M., Sawada, T., Tsuchida, Y., Voûte, P. A., Eds.; Elsevier Science BV: Amsterdam, 2000; p 582.
(2) Nishiher, H.; Toyoda, Y.; Tanaka, Y., et al. Natural corse of neuroblastoma detected by mass screening: a 5-year prospective study at a single institution. *J. Clin. Oncol.* **2000**, *18*, 3012−3017.
(3) Yamamoto, K.; Hanada, R.; Kikuchi, A.; Ichikawa, M.; Aihara, T.; Oguma, E.; Moritani, T.; Shimanuki, Y.; Tanimura, M.; Hayashi, Y. Spontaneous regression of localized neuroblastoma detected by mass screening. *J. Clin. Oncol.* **1998**, *16* (4), 1265−1269.
(4) (a) Castleberry. R. P. Pediatric update: neuroblastoma. *Eur. J. Cancer* **1997**, *33*, 1430−1438. (b) De Luca, L. M. Retinoids and their receptors in differentiation, embryogenesis, and neoplasia. *FASEB J.* **1991**, *5* (14), 2924−2933.
(5) Sidell, N. Retinoic acid-induced growth inhibition and morphologic differentiation of human neuroblastoma cells in vitro. *J. Natl. Cancer Inst.* **1982**, *68* (4), 589−596.
(6) Ludwig, K. W.; Lowey, B.; Niles, R. M. Retinoic acid increases cyclic AMP-dependent protein kinase activity in murine melanoma cells. *J. Biol. Chem.* **1980**, *255* (13), 5999−6002.
(7) Breitman, T. R.; Selonick, S. E.; Collins, S. J. Induction of differentiation of the human promyelocytic leukemia cell line (HL-60) by retinoic acid. *Proc. Natl. Acad. Sci. U.S.A.* **1980**, *77* (5), 2936−2940.
(8) Huang. M. E.; Ye. Y. C.; Chen. S. R.; Chai. J. R.; Lu. J. X.; Zhao. L.; Gu. L. J.; Wang. Z. Y. Use of all-trans retinoic acid in the treatment of acute promyelocytic leukemia. *Haematol. Blood Transfus.* **1989**, *32*, 88−96.
(9) Reynolds, C. P.; Matthay, K. K.; Villablanca, J. G.; Maurer, B. J. Retinoid therapy of high-risk neuroblastoma. *Cancer Lett.* **2003**, *197* (1−2), 185−192.
(10) Veal, G. J.; Errington, J.; Redfern, C. P.; Pearson, A. D.; Boddy, A. V. Influence of isomerisation on the growth inhibitory effects and cellular activity of 13-cis and all-trans retinoic acid in neuroblastoma cells. *Biochem. Pharmacol.* **2002**, *63* (2), 207−215.
(11) Reynolds, C. P.; Schindler, P. F.; Jones, D. M.; Gentile, J. L.; Proffitt, R. T.; Einhorn, P. A. Comparison of 13-cis-retinoic acid to trans-retinoic acid using human neuroblastoma cell lines. *Prog. Clin. Biol. Res.* **1994**, *385*, 237−244.
(12) Matthay, K. K.; Villablanca, J. G.; Seeger, R. C.; Stram ,D. O.; Harris, R. E.; Ramsay, N. K.; Swift, P.; Shimada, H.; Black, C. T.; Brodeur, G. M.; Gerbing, R. B.; Reynolds, C. P. Treatment of high-risk neuroblastoma with intensive chemotherapy, radiotherapy, autologous bone marrow transplantation, and 13-cis-retinoic acid. *Children's Cancer Group. N. Engl. J. Med.* **1999**, *341* (16), 1165−1173.

(13) Yuza, Y.; Agawa, M.; Matsuzaki, M.; Yamada, H.; Urashima, M. Gene and protein expression profiling during differentiation of neuroblastoma cells triggered by 13-cis retinoic acid. *J. Pediatr. Hematol. Oncol.* **2003**, *25* (9), 715−720.
(14) Sucov, H. M.; Evans, R. M. Retinoic acid and retinoic acid receptors in development. *Mol. Neurobiol.* **1995**, *10* (2−3), 169−184.
(15) Reynolds, C. P.; Kane, D. J.; Einhorn, P. A.; Matthay, K. K.; Crouse, V. L.; Wilbur, J. R.; Shurin, S. B.; Seeger, R. C. Response of neuroblastoma to retinoic acid in vitro and in vivo. *Prog. Clin. Biol. Res.* **1991**, *366*, 203−211.
(16) Ohira, M.; Morohashi, A.; Inuzuka, H.; Shishikura, T.; Kawamoto, T.; Kageyama, H.; Nakamura, Y.; Isogai, E.; Takayasu, H.; Sakiyama, S.; Suzuki, Y.; Sugano, S.; Goto, T.; Sato, S.; Nakagawara, A. Expression profiling and characterization of 4200 genes cloned from primary neuroblastomas: identification of 305 genes differentially expressed between favorable and unfavorable subsets. *Oncogene* **2003**, *22* (35), 5525−5536.
(17) Hiyama, E.; Hiyama, K.; Yamaoka, H.; Sueda, T.; Reynolds, C. P.; Yokoyama, T. Expression profiling of favorable and unfavorable neuroblastomas. *Pediatr. Surg. Int.* **2004**, *20* (1), 33−38.
(18) Ohira, M.; Oba, S.; Nakamura, Y.; Isogai, E.; Kaneko, S.; Nakagawa, A.; Hirata, T.; Kubo, H.; Goto, T.; Yamada, S.; Yoshida, Y.; Fuchioka, M.; Ishii, S.; Nakagawara, A. Expression profiling using a tumor-specific cDNA microarray predicts the prognosis of intermediate risk neuroblastomas. *Cancer Cell* **2005**, *7* (4), 337−350.
(19) Riley, R. D.; Heney, D.; Jones, D. R.; Sutton, A. J.; Lambert, P. C.; Abrams, K. R.; Young, B.; Wailoo, A. J.; Burchill, S. A. A systematic review of molecular and biological tumor markers in neuroblastoma. *Clin. Cancer Res.* **2004**, *10* (1 Pt 1), 4−12.
(20) Wei, J. S.; Greer, B. T.; Westermann, F.; Steinberg, S. M.; Son, C. G.; Chen, Q. R.; Whiteford, C. C.; Bilke, S.; Krasnoselsky, A. L.; Cenacchi, N.; Catchpoole, D.; Berthold, F.; Schwab, M.; Khan, J. Prediction of clinical outcome using gene expression profiling and artificial neural networks for patients with neuroblastoma. *Cancer Res.* **2004**, *64* (19), 6883−6891.
(21) Takita, J.; Ishii, M.; Tsutsumi, S.; Tanaka, Y.; Kato, K.; Toyoda, Y.; Hanada, R.; Yamamoto, K.; Hayashi, Y.; Aburatani, H. Gene expression profiling and identification of novel prognostic marker genes in neuroblastoma. *Genes, Chromosomes Cancer* **2004**, *40* (2), 120−132.
(22) Urbani, A.; Poland, J.; Bernardini, S.; Bellincampi, L.; Biroccio, A.; Schnolzer, M.; Sinha, P.; Federici, G. A proteomic investigation into etoposide chemo-resistance of neuroblastoma cell lines. *Proteomics* **2005**, *5*, (3), 796−804.
(23) Escobar, M. A.; Hoelz, D. J.; Sandoval, J. A.; Hickey, R. J.; Grosfeld, J. L.; Malkas, L. H. Profiling of nuclear extract proteins from human neuroblastoma cell lines: the search for fingerprints. *J. Pediatr. Surg.* **2005**, *40* (2), 349−358.
(24) Afjehi-Sadat, L.; Shin, J. H.; Felizardo, M.; Lee, K.; Slavc, I.; Lubec, G. Detection of hypothetical proteins in 10 individual human tumor cell lines. *Biochim. Biophys. Acta* **2005**, *1747* (1), 67−80.
(25) Marengo, E.; Robotti, E.; Righetti, P. G.; Campostrini, N.; Pascali, J.; Ponzoni, M.; Hamdan, M.; Astner, H. Study of proteomic changes associated with healthy and tumoral murine samples in neuroblastoma by principal component analysis and classification methods. *Clin. Chim. Acta* **2004**, *345*, (1−2), 55−67.
(26) Campostrini, N.; Pascali, J.; Hamdan, M.; Astner, H.; Marimpietri, D.; Pastorino, F.; Ponzoni, M.; Righetti, P. G. Proteomic analysis of an orthotopic neuroblastoma xenograft animal model. *J. Chromatogr., B: Anal. Technol. Biomed. Life Sci.* **2004**, *808* (2), 279−286.
(27) Harris, M. N.; Ozpolat, B.; Abdi, F.; Gu, S.; Legler, A.; Mawuenyega, K. G.; Tirado-Gomez, M.; Lopez-Berestein, G.; Chen, X. Comparative proteomic analysis of all-trans-retinoic acid treatment reveals systematic posttranscriptional control mechanisms in acute promyelocytic leukemia. *Blood* **2004**, *104* (5), 1314−1323.
(28) Zheng, P. Z.; Wang, K. K.; Zhang, Q. Y.; Huang, Q. H.; Du, Y. Z.; Zhang, Q. H.; Xiao, D. K.; Shen, S. H.; Imbeaud, S.; Eveno, E.; Zhao, C. J.; Chen, Y. L.; Fan, H. Y. Waxman, S.; Auffray, C.; Jin, G.; Chen, S. J.; Chen, Z.; Zhang, J. Systems analysis of transcriptome and proteome in retinoic acid/arsenic trioxide-induced cell differentiation/apoptosis of promyelocytic leukemia. *Proc. Natl. Acad. Sci. U.S.A.* **2005**, *102* (21), 7653−7658.
(29) Guo, X.; Ying, W.; Wan, J.; Hu, Z.; Qian, X.; Zhang, H.; He, F. Proteomic characterization of early-stage differentiation of mouse embryonic stem cells into neural cells induced by all-trans retinoic acid in vitro. *Electrophoresis* **2001**, (14), 3067−3075.
(30) Tonge, R.; Shaw, J.; Middleton, B.; Rowlinson, R.; Rayner, S.; Young, J.; Pognan, F.; Hawkins, E.; Currie, I.; Davison, M. Validation and development of fluorescence two-dimensional differential gel electrophoresis proteomics technology. *Proteomics* **2001**, *1* (3), 377−396.
(31) Friedman, D. B.; Hill, S.; Keller, J. W.; Merchant, N. B.; Levy, S. E.; Coffey, R. J.; Caprioli, R. M. Proteome analysis of human colon cancer by two-dimensional difference gel electrophoresis and mass spectrometry. *Proteomics* **2004**, *4* (3), 793−811.
(32) Zhou, G.; Li, H.; DeCamp, D.; Chen, S.; Shu, H.; Gong, Y.; Flaig, M.; Gillespie, J. W.; Hu, N.; Taylor, P. R.; Emmert-Buck, M. R.; Liotta, L. A.; Petricoin, E. F., 3rd; Zhao, Y. 2D differential in-gel electrophoresis for the identification of esophageal scans cell cancer-specific protein markers. *Mol. Cell. Proteomics* **2002**, *1* (2), 117−124.
(33) Somiari, R. I.; Sullivan, A.; Russell, S.; Somiari, S.; Hu, H.; Jordan, R.; George, A.; Katenhusen, R.; Buchowiecka, A.; Arciero, C.; Brzeski, H.; Hooke, J.; Shriver, C. High-throughput proteomic analysis of human infiltrating ductal carcinoma of the breast. *Proteomics* **2003**, *3* (10), 1863−1873.
(34) Hoorn, E. J.; Hoffert, J. D.; Knepper, M. A. The application of DIGE-based proteomics to renal physiology. *Nephron Physiol.* **2006**, *104* (1), 61−72.
(35) Herrero, J.; Al-Shahrour, F.; Díaz-Uriarte, R.; Mateos, Á.; Vaquerizas, J. M.; Santoyo, J.; Dopazo, J. GEPAS, a web-based resource for microarray gene expression data analysis. *Nucleic Acids Res.* **2003**, *31* (13), 3461−3467.
(36) Herrero, J.; Vaquerizas, J. M.; Al-Shahrour, F.; Conde, L.; Mateos, Á.; Santoyo, J.; Díaz-Uriarte, R.; Dopazo, J. New challenges in gene expression data analysis and the extended GEPAS. *Nucleic Acids Res.* **2004**, *32* (W485−W491).
(37) Cesi, V.; Tanno, B.; Vitali, R.; Mancini, C.; Giuffrida, M. L.; Calabretta, B.; Raschella, G. Cyclin D1-dependent regulation of B-myb activity in early stages of neuroblastoma differentiation. *Cell Death Differ.* **2002**, *9* (11), 1232−1239.
(38) Hettmer, S.; McCarter, R.; Ladisch, S.; Kaucic, K. Alterations in neuroblastoma ganglioside synthesis by induction of GD1b synthase by retinoic acid. *Br. J. Cancer* **2004**, *91* (2), 389−397.
(39) Villablanca, J. G.; Khan, A. A.; Avramis, V. I.; Seeger, R. C.; Matthay, K. K.; Ramsay, N. K.; Reynolds, C. P. Phase I trial of 13-cis-retinoic acid in children with neuroblastoma following bone marrow transplantation. *J. Clin. Oncol.* **1995**, *13* (4), 894−901.
(40) Pagani, A.; Forni, M.; Tonini, G. P.; Papotti, M.; Bussolati, G. Expression of members of the chromogranin family in primary neuroblastomas. *Diagn. Mol. Pathol.* **1992**, *1* (1), 16−24.
(41) Giudici, A. M.; Sher, E.; Pelagi, M.; Clementi, F.; Zanini, A. Immunolocalization of secretogranin II, chromogranin A, and chromogranin B in differentiating human neuroblastoma cells. *Eur. J. Cell Biol.* **1992**, *58* (2), 383−389.
(42) Jang, Y. K.; Park, J. J.; Lee, M. C.; Yoon, B. H.; Yang, Y. S.; Yang, S. E.; Kim, S. U. Retinoic acid-mediated induction of neurons and glial cells from human umbilical cord-derived hematopoietic stem cells. *J. Neurosci. Res.* **2004**, *75* (4), 573−584.
(43) Keim, D. R.; Hailat, N.; Kuick, R.; Reynolds, C. P.; Brodeur, G. M.; Seeger, R. C.; Hanash, S. M. PCNA levels in neuroblastoma are increased in tumors with an amplified N-myc gene and in metastatic stage tumors. *Clin. Exp. Metastasis* **1993**, *11* (1), 83−90.
(44) Mejia, C.; Navarro, S.; Pellin, A.; Ruiz, A.; Castel, V.; Llombart-Bosch, A. Prognostic significance of cell proliferation in human neuroblastoma: comparison with other prognostic factors. *Oncol. Rep.* **2003**, *10* (1), 243−247.
(45) Duncan, R.; Bazar, L.; Michelotti, G.; Tomonaga, T.; Krutzsch, H.; Avigan, M.; Levens, D. A sequence-specific, single-strand binding protein activates the far upstream element of c-myc and defines a new DNA-binding motif. *Genes Dev.* **1994**, *8* (4), 465−480.
(46) Tao, W.; Wang, M.; Voss, E. D.; Cocklin, R. R.; Smith, J. A.; Cooper, S. H.; Broxmeyer, H. E. Comparative proteomic analysis of human CD34+ stem/progenitor cells and mature CD15+ myeloid cells. *Stem Cells* **2004**, *22* (6), 1003−1014.
(47) Bown, N. Neuroblastoma tumour genetics: clinical and biological aspects. *J. Clin. Pathol.* **2001**, *54* (12), 897−910.
(48) Maris, J. M.; Matthay, K. K. Molecular biology of neuroblastoma. *J. Clin. Oncol.* **1999**, *17* (7), 2264−2279.
(49) Mora, J.; Cheung, N. K.; Oplanich, S.; Chen, L.; Gerald, W. L. Novel regions of allelic imbalance identified by genome-wide analysis of neuroblastoma. *Cancer Res.* **2002**, *62* (6), 1761−1767.

(50) Mosse, Y. P.; Greshock, J.; Margolin, A.; Naylor, T.; Cole, K.; Khazi, D.; Hii, G.; Winter, C.; Shahzad, S.; Asziz, M. U.; Biegel, J. A.; Weber, B. L.; Maris, J. M. High-resolution detection and mapping of genomic DNA alterations in neuroblastoma. *Genes, Chromosomes Cancer* **2005**, *43* (4), 390−403.
(51) Chen, Q. R.; Bilke, S.; Wei, J. S.; Whiteford, C. C.; Cenacchi, N.; Krasnoselsky, A. L.; Greer, B. T.; Son, C. G.; Westermann, F.; Berthold, F.; Schwab, M.; Catchpoole, D.; Khan, J. cDNA array-CGH profiling identifies genomic alterations specific to stage and MYCN-amplification in neuroblastoma. *BMC Genomics* **2004**, *5* (1), 7.
(52) Hackett, C. S.; Hodgson, J. G.; Law, M. E.; Fridly, J.; Osoegawa, K.; de Jong, P. J.; Nowak, N. J.; Pinkel, D.; Albertson, D. G.; Jain, A.; Jenkins, R.; Gray, J. W.; Weiss, W. A. Genome-wide array CGH analysis of murine neuroblastoma reveals distinct genomic aberrations which parallel those in human tumors. *Cancer Res.* **2003**, *63* (17), 5266−5273.
(53) Poon, H. F.; Shepherd, H. M.; Reed, T. T.; Calabrese, V.; Stella, A. M.; Pennisi, G.; Cai, J.; Pierce, W. M.; Klein, J. B.; Butterfield, D. A. Proteomics analysis provides insight into caloric restriction mediated oxidation and expression of brain proteins associated with age-related impaired cellular processes: Mitochondrial dysfunction, glutamate dysregulation and impaired protein synthesis. *Neurobiol. Aging* **2006**, *27* (7), 1020−1034.
(54) Godbout, R.; Packer, M.; Bie, W. Overexpression of a DEAD box protein (DDX1) in neuroblastoma and retinoblastoma cell lines. *J. Biol. Chem.* **1998**, *273* (33), 21161−21168.
(55) Pandita, A.; Godbout, R.; Zielenska, M.; Thorner, P.; Bayani, J.; Squire, J. A. Relational mapping of MYCN and DDXI in band 2p24 and analysis of amplicon arrays in double minute chromosomes and homogeneously staining regions by use of free chromatin FISH. *Genes, Chromosomes Cancer* **1997**, *20* (3), 243−252.
(56) Manohar, C. F.; Salwen, H. R.; Brodeur, G. M.; Cohn, S. L. Co-amplification and concomitant high levels of expression of a DEAD box gene with MYCN in human neuroblastoma. *Genes, Chromosomes Cancer* **1995**, *14* (3), 196−203.
(57) Squire, J. A.; Thorner, P. S.; Weitzman, S.; Maggi, J. D.; Dirks, P.; Doyle, J.; Hale, M.; Godbout, R. Co-amplification of MYCN and a DEAD box gene (DDX1) in primary neuroblastoma. *Oncogene* **1995**, *10* (7), 1417−1422.
(58) George, R. E.; Kenyon, R. M.; McGuckin, A. G.; Malcolm, A. J.; Pearson, A. D.; Lunec, J. Investigation of co-amplification of the candidate genes ornithine decarboxylase, ribonucleotide reductase, syndecan-1 and a DEAD box gene, DDX1, with N-myc in neuroblastoma. United Kingdom Children's Cancer Study Group. *Oncogene* **1996**, *12* (7), 1583−1587.
(59) Scott, D.; Elsden, J.; Pearson, A.; Lunec, J. Genes co-amplified with MYCN in neuroblastoma: silent passengers or co-determinants of phenotype? *Cancer Lett.* **2003**, *197* (1−2), 81−86.
(60) Bleoo, S.; Sun, X.; Hendzel, M. J.; Rowe, J. M.; Packer, M.; Godbout, R. Association of human DEAD box protein DDX1 with a cleavage stimulation factor involved in 3′-end processing of pre-MRNA. *Mol. Biol. Cell.* **2001**, *12* (10), 3046−3059.
(61) Stratford, A. L.; Boelaert, K.; Tannahill, L. A.; Kim, D. S.; Warfield, A.; Eggo, M. C. Gittoes, N. J.; Young, L. S.; Franklyn, J. A.; McCabe, C. J. Pituitary tumor transforming gene binding factor: a novel transforming gene in thyroid tumorigenesis. *J. Clin. Endocrinol. Metab.* **2005**, *90* (7), 4341−4349.
(62) Balasubramani, M.; Day, B. W.; Schoen, R. E.; Getzenberg, R. H. Altered expression and localization of creatine kinase B, heterogeneous nuclear ribonucleoprotein F, and high mobility group box 1 protein in the nuclear matrix associated with colon cancer. *Cancer Res.* **2006**, *66* (2), 763−769.
(63) Eberle, J.; Krasagakis, K.; Orfanos, C. E. Translation initiation factor eIF-4A1 mRNA is consistently overexpressed in human melanoma cells in vitro. *Int. J. Cancer* **1997**, *71* (3), 396−401.
(64) Shuda, M.; Kondoh, N.; Tanaka, K.; Ryo, A.; Wakatsuki, T.; Hada, A.; Goseki, N.; Igari, T.; Hatsuse, K.; Aihara, T.; Horiuchi, S.; Shichita, M.; Yamamoto, N.; Yamamoto, M. Enhanced expression of translation factor mRNAs in hepatocellular carcinoma. *Anticancer Res.* **2000**, *20* (4), 2489−2489.
(65) Yoon, S. Y.; Kim, J. M.; Oh, J. H.; Jeon, Y. J.; Lee, D. S.; Kim, J. H.; Choi, J. Y.; Ahn, B. M.; Kim, S.; Yoo, H. S.; Kim, Y. S.; Kim, N. S. Gene expression profiling of human HBV- and/or HCV-associated hepatocellular carcinoma cells using expressed sequence tags. *Int. J. Oncol.* **2006**, *29* (2), 315−327.
(66) Ji, P.; Diederichs, S.; Wang, W.; Boing, S.; Metzger, R.; Schneider, P. M.; Tidow, N.; Brandt, B.; Buerger, H.; Bulk, E.; Thomas, M.; Berdel, W. E.; Serve, H.; Muller-Tidow, C. MALAT-1, a novel noncoding RNA, and thymosin beta4 predict metastasis and survival in early-stage non-small cell lung cancer. *Oncogene* **2003**, *22* (39), 8031−8041.
(67) Biedler, J. L.; Helson, L.; Spengler, B. A. Morphology and growth, tumorigenicity, and cytogenetics of human neuroblastoma cells in continuous culture. *Cancer Res.* **1973**, *33* (11), 2643−2652.
(68) Biedler, J. L.; Spengler, B. A. A novel chromosome abnormality in human neuroblastoma and antifolate-resistant Chinese hamster cell lives in culture. *J. Natl. Cancer Inst.* **1976**, *57* (3), 683−695.
(69) Bordow, S. B.; Norris, M. D.; Haber, P. S.; Marshall, G. M.; Haber, M. Prognostic significance of MYCN oncogene expression in childhood neuroblastoma. *J. Clin. Oncol.* **1998**, *16* (10), 3286−3294
(70) Nguyen, T.; Hocker, J. E.; Thomas, W.; Smith, S. A.; Norris, M. D.; Haber, M.; Cheung, B.; Marshall, G. M. Combined RAR alpha- and RXR-specific ligands overcome N-myc-associated retinoid resistance in neuroblastoma cells. *Biochem. Biophys. Res. Commun.* **2003**, *302* (3), 462−468.
(71) Oh, J. E.; Karlmark, K. R.; Shin, J.; Hengstschlager, M.; Lubec, G. Differentiation-dependent expression of hypothetical proteins in the neuroblastoma cell line N1E-115. *Proteins* **2006**, *63* (3), 671−680.
(72) Woodward, E. R.; Buchberger, A.; Clifford, S. C.; Hurst, L. D.; Affara, N. A.; Maher, E. R. Comparative sequence analysis of the VHL tumor suppressor gene. *Genomics* **2000**, *65* (3) 253−265.
(73) Brinke, A.; Green, P. M.; Giannelli, F. Characterization of the gene (VBP1) and transcript for the von Hippel-Lindau binding protein and isolation of the highly conserved murine homologue. *Genomics* **1997**1, *45* (1), 105−112.
(74) Iwai, K.; Yamanaka, K.; Kamura, T.; Minato, N.; Conaway, R. C.; Conaway, J. W.; Klausner, R. D.; Pause, A. Identification of the von Hippel-lindau tumor-suppressor protein as part of an active E3 ubiquitin ligase complex. *Proc. Natl. Acad. Sci. U.S.A.* **1999**, *96* (22), 12436−12441.
(75) Lisztwan, J.; Imbert, G.; Wirbelauer, C.; Gstaiger, M.; Krek, W. The von Hippel-Lindau tumor suppressor protein is a component of an E3 ubiquitin-protein ligase activity. *Genes Dev.* **1999**, *13* (14), 1822−1833.
(76) Maxwell, P. H.; Wiesener, M. S.; Chang, G. W.; Clifford, S. C.; Vaux, E. C.; Cockman, M. E.; Wykoff, C. C.; Pugh, C. W.; Maher, E. R.; Ratcliffe, P. J. Hypoxia-inducible factors for oxygen-dependent proteolysis. *Nature* **1999**, *399* (6733), 271−275.
(77) Gnarra, J. R.; Duan, D. R.; Weng, Y.; Humphrey, J. S.; Chen, D. Y.; Lee, S.; Pause, A.; Dudley, C. F.; Latif, F.; Kuzmin, I.; Schmidt, L.; Duh, F. M.; Stackhouse, T.; Chen, F.; Kishida, T.; Wei, M. H.; Lerman, M. I.; Zbar, B.; Klausner, R. D.; Linehan, W. M. Molecular cloning of the von Hippel-Lindau tumor suppressor gene and its role in renal carcinoma. *Biochim. Biophys. Acta* **1996**, *1242* (3), 201−210.
(78) Spitz, R.; Hero, B.; Ernestus, K.; Berthold, F. FISH analyses for alterations in chromosomes 1, 2, 3, and 11 define high-risk groups in neuroblastoma. *Med. Pediatr. Oncol.* **2003**, *41* (1), 30−35.
(79) Hoebeeck, J.; Vandesompele, J.; Nilsson, H.; De Preter, K.; Van Roy, N.; De Smet, E.; Yigit, N.; De Paepe, A.; Laureys, G.; Pahlman, S.; Speleman, F. The von Hippel-Lindau tumor suppressor gene expression level has prognostic value in neuroblastoma. *Int. J. Cancer* **2006**, *119* (3), 624−629.
(80) Murata, H.; Tajima, N.; Nagashima, Y.; Yao, M.; Baba, M.; Goto, M.; Kawamoto, S.; Yamamoto, I.; Okuda, K.; Kanno, H. Von Hippel-Lindau tumor suppressor protein transforms human neuroblastoma cells into functional neuron-like cells. *Cancer Res.* **2002**, *62* (23), 7004−7011.
(81) Kanno, H.; Saljooque, F.; Yamamoto, I.; Hattori, S.; Yao, M.; Shuin, T.; U, H. S. Role of the von Hippel-Lindau tumor suppressor protein during neuronal differentiation. *Cancer Res.* **2000**, *60* (11), 2820−2824.
(82) Tsuchiya, H.; Iseda, T.; Hino, O. Identification of a novel protein (VBP-1) binding to the von Hippel-Lindau (VHL) tumor suppressor gene product. *Cancer Res.* **1996**, *56* (13), 2881−2885.

PR060701G